Catal Lett (2008) 124:288–296
DOI 10.1007/s10562-008-9451-3

ORIGINAL PAPER

# A Comparison Study on the Structure and Performance of Mo–V–O and Mo–V–Te–O Catalysts Synthesized Hydrothermally with Ultrasonic Pretreatment for Propane Oxidation

**Xiujuan Yang · Weifeng Zhang · Ruming Feng · Weijie Ji · Chak-Tong Au**

Received: 18 December 2007 / Accepted: 21 February 2008 / Published online: 11 March 2008


**Abstract** The $Mo_{1.00}V_{0.80}O_n$ and $Mo_{1.00}V_{\alpha}Te_{0.17}O_n$ ($\alpha = 0.40$–$1.00$) catalysts were prepared hydrothermally with ultrasonic pretreatment for propane partial oxidation. The fabricated catalysts were characterized by BET, XRD, Raman, XPS, EPR, SEM, $H_2$–TPR, and $NH_3$-calorimetric techniques. It is revealed that the content of vanadium in the catalysts is crucial for the generation of phase structure essential for good performance. The role of Te in the catalytic system and the effect of ultrasonic treatment during catalyst fabrication on catalyst properties are interpreted based on the characterization and reaction results obtained.

**Keywords** Selective oxidation · Propane · Mixed metal oxide · Ultrasonic and hydrothermal treatments

## 1 Introduction

The selective oxidation of light alkanes ($C_1$–$C_4$) to valuable oxygenated products has been investigated extensively in both industrial and academic sectors. Despite lots of efforts, only the partial oxidation of *n*-butane to maleic anhydride over vanadium phosphorus oxide catalysts has been industrialized [1]. The main challenge in the partial oxidation of light alkanes is how to activate the relatively s3 C–H bonds of light alkanes while having the cleavage of C–C bonds and deep oxidation of intermediates and desired products properly suppressed.

Acrylic acid (AA) is an important and versatile chemical. It is produced industrially by the oxidation of propylene with acrolein being an intermediate [2]. In terms of economic and enviromential consideration, it is highly desireable to obtain AA directly from propane, and the one-step oxidation of propane to AA has attracted vast attention worldwide. Catalysts such as vanadium phosphorus oxide [3, 4], heteropolyacids [5], and mixed metal oxides (MMO) [6–30] have been investigated for this purpose. There are generally two types of mixed metal oxide (MMO) catalysts effective for the direct oxidation of propane to acrylic acid, namely, Mo–V–Te–O and Mo–V–Te–Nb–O, respectively. Generally speaking, inclusion of Nb component into the Mo–V–Te–O system can further enhance catalyst performance [7]. Note that, however, MMO catalyst performance is strongly dependent on elemental composition of catalyst (even for the Mo–V–Te–O) as well as catalyst preparation methodology [8–17], and the "window" of obtaining an active catalyst is rather narrow [18, 19]. In addition, the Mo–V–Te–O system is a basis of the Mo–V–Te–Nb–O one. Investigation of the former system is no doubt helpful for better understanding the function of Nb component in the Mo–V–Te–Nb–O system.

It has been demonstrated that the method of hydrothermal synthesis is suitable for the generation of MMOs with large surface area and discrete phase composition [20–30]. Our previous studies demonstrated the effectiveness of the hydrothermal synthesis approach with ultrasonic pretreatment to the MMO catalytic system [25, 31]. In the present study, we applied the same synthesis strategy to two-component (Mo–V–O) and three-component (Mo–V–Te–O)

X. Yang · W. Zhang · R. Feng · W. Ji (✉)
Key Laboratory of Mesoscopic Chemistry, Ministry of Education, School of Chemistry and Chemical Engineering, Nanjing University, Nanjing 210093, China
e-mail: jiwj@nju.edu.cn

X. Yang · C.-T. Au (✉)
Department of Chemistry, Center for Surface Analysis and Research, Hong Kong Baptist University, Kowloon Tong, Hong Kong, China
e-mail: pctau@hkbu.edu.hk

catalysts with a variety of V concentration. The Mo–V–O/Mo–V–Te–O catalysts of different V-content fabricated via ultrasonic-hydrothermal treatment are exclusive and of interest to study. Since the use of $TeO_2$ as Te source is much effective than telluric acid for generation of active Mo–V–Te–O catalyst; the application of ultrasonic treatment to enhance $TeO_2$ dispersion in preparing a serial Mo–V–Te–O catalysts with different V content is indeed helpful. On the other hand, telluric acid was found to be superior to $TeO_2$ as Te source for preparation of Mo–V–Te–Nb–O catalyst. However, our recent study indicated that a $TeO_2$-derived Mo–V–Te–Nb–O catalyst prepared with a proper ultrasonic treatment can perform better than the $H_6TeO_6$-derived counterpart [31]. The study on the addition of Te in Mo–V–O and the systematic regulation of V content in Mo–V–Te–O with an ultrasonic-assisted preparation can provide new insights into the roles of enhanced $TeO_2$ dispersion and variable V content in the generation of efficient Mo–V–Te–O catalyst for the target reaction.

## 2 Experimental

### 2.1 Preparation of Catalysts

The starting materials were purchased from Aldrich Chemical Company and used without further purification. The ultrasonic pretreatment applied to the reaction mixture was to enhance the interaction between the catalyst constituents [25]. For the generation of the Mo–V–O catalyst, ammonium paramolybdate tetrahydrate (4.50 g) was added to de-ionized (DI) water, and with constant stirring a designated amount of vanadyl sulfate solution (1.0 mol $L^{-1}$) was added drop-wise. The mixture so-obtained is denoted as "Mo–V". For the generation of the three-component catalysts, ammonium paramolybdate tetrahydrate (4.50 g) and $TeO_2$ powder (0.81 g) were mixed in DI water and a designated amount of vanadyl sulfate solution (1.0 mol $L^{-1}$) was added drop-wise to the resulting suspension containing paramolybdate tetrahydrate and $TeO_2$ under a 40-min ultrasonic treatment (80 W at 40 kHz; KQ 2200 DE, Kuen Shan Ultrasonic Instrument Co., Ltd., China) (the mixture so-obtained is denoted as "Mo–V–Te"). The "Mo–V" and "Mo–V–Te" mixtures were subject to ca. 40 min of ultrasonic treatment before being treated hydrothermally in a Teflon-lined stainless steel autoclave at 175 °C for 72 h. The resulting solid was filtered out, washed with DI water, and dried at 80 °C for 12 h. The precursor so obtained was activated in static argon at 600 °C for 2 h after being heated (at a rate of 5 °C/min in a covered quartz crucible under Ar) from room temperature (RT) to 600 °C. The resulting solids were ground, pressed, crushed, and sieved to 20–40 mesh for use.

There are totally six fabricated catalysts, and their characteristics are depicted in Tables 1–4. Catalyst A has a nominal composition of $Mo_{1.00}V_{0.80}O_n$ whereas catalysts B to E can be represented nominally as $Mo_{1.00}V_{\alpha}Te_{0.17}O_n$ ($\alpha = 0.40$–$1.00$). Catalyst C* is similar to catalyst C in composition but was prepared without the ultrasonic treatment. For all of the catalysts, the content of V, Te is normalized against that of Mo (Table 2).

### 2.2 Catalysts Characterization

The activated catalysts were characterized by specific surface area (BET) measurement, X-ray fluorescence

**Table 1** BET surface area and performance data of catalysts[a]

| Catalyst | BET ($m^2/g$) | AA Yield (%) | $C_3$ Conv. (%) | Selectivity (%) | | | | |
|---|---|---|---|---|---|---|---|---|
| | | | | AA | ACR[b] | ACOH[c] | $C_3H_6$ | $CO_x$ |
| A-$Mo_{1.00}V^{d}_{0.80}$ | 7.0 | Trace | 10.5 | 1.9 | 2.6 | 0 | 63.1 | 32.5 |
| B-$Mo_{1.00}V_{0.40}Te_{0.17}$ | 3.8 | 5.3 | 13.2 | 40.2 | 0.4 | 5.1 | 19.6 | 34.8 |
| C-$Mo_{1.00}V_{0.60}Te_{0.17}$ | 3.9 | 14.1 | 48.4 | 29.0 | 0.3 | 11.9 | 5.5 | 53.2 |
| C*-$Mo_{1.00}V_{0.60}Te^{e}_{0.17}$ | 4.7 | 7.9 | 48.9 | 16.1 | 0.1 | 4.7 | 5.1 | 74.0 |
| D-$Mo_{1.00}V_{0.80}Te_{0.17}$ | 6.4 | 17.4 | 46.7 | 37.2 | 0.1 | 10.3 | 5.7 | 46.7 |
| E-$Mo_{1.00}V_{1.00}Te_{0.17}$ | 2.9 | Trace | 39.5 | Trace | 0.6 | 0 | 17.8 | 81.5 |
| E-$Mo_{1.00}V_{1.00}Te^{f}_{0.17}$ | 2.9 | Trace | 4.8 | Trace | 45.7 | 4.9 | 43.9 | 5.5 |

[a] Reaction feed: propane/oxygen/steam/helium = 6/12/40/42 (v/v/v/v), catalyst amount: 1 g, W/F = 249 $g_{cat}$ h (mol $_{C3H8}$)$^{-1}$, reaction temperature = 400 °C unless indicated otherwise

[b] ACR: acrolein

[c] ACOH: acetic acid

[d] Reaction conducted at 380 °C

[e] Catalyst C* was prepared without ultrasonic treatment

[f] Reaction conducted at 260 °C

**Table 2** Components (Mo/V/Te) characterization of calcined Mo–V–Te–O catalysts

| Nominal composition | Measured bulk composition[a] | Surface composition[b] |
|---|---|---|
| B-$Mo_{1.00}V_{0.40}Te_{0.167}$ | 1.00/0.23/0.14 | / |
| C-$Mo_{1.00}V_{0.60}Te_{0.167}$ | 1.00/0.53/0.16 | 1.00/0.31/0.25 |
| C*-$Mo_{1.00}V_{0.60}Te_{0.167}$ | 1.00/0.55/0.15 | 1.00/0.32/0.21 |
| D-$Mo_{1.00}V_{0.80}Te_{0.167}$ | 1.00/0.92/0.30 | 1.00/0.33/0.18 |
| E-$Mo_{1.00}V_{1.00}Te_{0.167}$ | 1.00/0.95/0.31 | 1.00/0.38/0.19 |

[a] Determined by XRF

[b] Determined by XPS

**Table 3** XPS binding energies (eV) of Mo, V, and Te elements

| Catalyst | Mo3 $d_{5/2}$ | V2 $p_{3/2}$ | Te3 $d_{5/2}$ |
|---|---|---|---|
| C-$Mo_{1.00}V_{0.60}Te_{0.17}$ | 232.5 | 516.3 | 576.3 |
| C*-$Mo_{1.00}V_{0.60}Te_{0.17}$ | 232.4 | 516.3 | 576.0 |
| D-$Mo_{1.00}V_{0.80}Te_{0.17}$ | 232.7 | 516.4 | 576.1 |
| E-$Mo_{1.00}V_{1.00}Te_{0.17}$ | 232.8 | 516.7 | 576.4 |

(XRF), X-ray diffraction (XRD), Raman, X-ray photoelectron spectroscopy (XPS), Electron spin resonance (ESR), Scanning electron microscopy (SEM), Hydrogen-temperature programmed reduction ($H_2$-TPR), and $NH_3$-microcalorimetric measurement. The BET measurement was conducted on a NOVA 1200 apparatus with $N_2$ adsorption at 77 K. The XRF measurement was carried out on an ARL-9800 XRF spectrometer. Catalyst phase composition was identified by XRD over an X' TRA X-ray diffractometer (equipped with a graphite monochromator) operated at 40 kV and 40 mA; the radiation was Cu K$\alpha$ ($\lambda = 0.1542$ nm) and the $2\theta$ range was 3–60°. Raman spectra were collected using an InVia Raman spectrometer (Renishaw Corporation) equipped with a laser source of 514 nm. XPS measurement was performed on a VG ESCALAB MK II instrument using Mg K$\alpha$ radiation (1253.6 eV); the high voltage and emission current was 12 kV and 20 mA, respectively. The surface elemental composition of samples was calculated with the corresponding peak areas normalized with reference to the Wagner Factor database. The relative experimental uncertainty of this quantitative analysis is considered to be about 10%. The binding energies (BEs) were calibrated against the C 1*s* (284.6 eV) peak of contaminant carbon. The ESR spectra were acquired on a JES-TE100 ESR spectrometer operated at the frequency of X-band mode at 77 K; the samples (10 mg) were placed in a quartz cell and the modulated frequency was 100 kHz. The SEM images of samples were acquired on a FEI QUANTA200 instrument. $H_2$-TPR was carried out within RT-800 °C range; 10 mg of sample was first pretreated in a flow of 5%$H_2$/Ar (40 mL/min) at 200 °C for 1 h and then reduced in the same atmosphere at a heating rate of 5 °C/min. $NH_3$-calorimetric measurement was performed on a Tian-Calvet heat flux apparatus. The catalysts were out-gassed at 300 °C for 1 h before ammonia adsorption.

### 2.3 Catalytic Performance

Selective oxidation of propane to AA was carried out at atmospheric pressure in a conventional fixed-bed Pyrex tubular reactor (Internal diameter = 8 mm) in the temperature range of 340–420 °C. The typical amount of charged catalyst was 1.0 g, and the reaction feed was propane/oxygen/steam/helium = 6/12/40/42 (volume ratio). The gas hourly space velocity (GHSV) was 1500 mL/(h $g_{cat}$). The corresponding W/F was 249 $g_{cat}$ h (mol $C_3H_8$)$^{-1}$. The reactants and products were analyzed by on-line GC system using a HP FFAP capillary column (25 m × 3 mm) for propane and oxygenates separation, a packed Hayesep D HP column (4 m × 3 mm) for $O_2$ (CO), $CO_2$, $C_3$ = and $C_3$ separation, and a packed 5A molecular sieve column (2 m × 3 mm) for $O_2$ and CO separation.

## 3 Results

### 3.1 BET, XRF, and XPS

As depicted in Table 1, the surface area of A-$Mo_{1.00}V_{0.80}$ sample is 7.0 $m^2$ $g^{-1}$. Across the serial catalysts B–D

**Table 4** Surface elemental compositions and Mo3 $d_{5/2}$, V2 $p_{3/2}$, and Te3 $d_{5/2}$ binding energies of catalyst D ($Mo_{1.00}V_{0.80}Te_{0.167}$) before and after calcination as well as after reaction

| State | Surface composition (mole ratio) | Binding energy (eV) | | |
|---|---|---|---|---|
| | | Mo3 $d_{5/2}$ | V2 $p_{3/2}$ | Te3 $d_{5/2}$ |
| Before calcination | 1.00/0.36/0.20 | 232.5 | 516.5 | 576.0 |
| After calcination | 1.00/0.33/0.18 | 232.7 | 516.4 | 576.1 |
| After reaction | 1.00/0.22/0.19 | 232.5 | 516.0 | 576.0 |

(Mo–$V_{\alpha}$–Te) with increasing V content ($\alpha = 0.40$–$0.80$), there is an increase in surface area from 3.8 to 6.4 $m^2\ g^{-1}$. The catalyst E with the highest V content ($\alpha = 1.00$) is the lowest in surface area (2.9 $m^2\ g^{-1}$). It is observed that the ultrasonic treatment has little effect on the surface area of the Mo–V–Te catalysts (i.e. C vs. C*).

The bulk (as determined by XRF) and surface elemental compositions (as measured by XPS) of the catalysts are given in Table 2. One can see that measured bulk and surface V content increases with nominal values. However, the surface elemental composition is different from the nominal and bulk ones. It is detected that the surface becomes more depleted of V at high nominal V contents, while the bulk V content is higher than the nominal value. It is apparent that there is loss of Mo and V during the hydrothermal process, and loss of Mo component could be more significant at higher V content, resulting in higher bulk composition of V/Mo and Te/Mo. Table 2 indicates that catalyst C is higher in Te surface concentration than catalyst C*. Our study on Mo–V–Te–Nb catalysts prepared with ultrasonic pretreatment also showed this tendency [31]. This could be due to the enhanced dispersion and interaction of $TeO_2$ with Mo and V constituents as a result of ultrasonic treatment. Moreover, the surface concentration of Te is also related to the V content of samples. On catalysts D and E, the Te surface concentrations are similar to the nominal values.

The XPS results of the activated catalysts are presented in Tables 3 and 4. The Mo3 $d_{5/2}$ BE of the Mo species is in the range of 232.3–232.8 eV, suggesting that both $Mo^{6+}$ and $Mo^{5+}$ could be present in the samples [27]. Note that, however, the apparent Mo3 $d_{5/2}$ BE cannot clearly tell the relative content of $Mo^{6+}$ and $Mo^{5+}$ in the various catalysts; this is because there are different phases in the samples, and the Mo3 $d_{5/2}$ BE of $Mo^{6+}$ or $Mo^{5+}$ could be different in the phases of $MoO_x$, M1/M2, and $VOMoO_4$. The result of ESR investigation (Sect. 3.2) confirmed this presumption. The Te3 $d_{5/2}$ BE of $TeO_2$ is 576.2 eV and that of $H_6TeO_6$ is 577.3 eV [32, 33]. It can be deduced from Table 3 that most of the surface Te species (Te3 $d_{5/2}$ BE = ca. 576 eV) are in oxidation state of +4. The V2 $p_{3/2}$ binding energy shifts from 516.3 to 516.7 eV with rise in V content of $Mo_{1.00}V_{\alpha}Te_{0.17}$ from $\alpha = 0.6$ to 1.0. The V2 $p_{3/2}$ binding energy of $V_2O_5$ and $VO_2$ (reference compounds) are 517.0 and 516.0 eV, respectively. Again, the content of $V^{5+}$ and $V^{4+}$ can be varied depending upon the elemental as well as phase composition of the samples. As indicated in Table 4, the Mo3 $d_{5/2}$, V2 $p_{3/2}$, and Te3 $d_{5/2}$ BEs of catalyst D detected before and after calcination are rather similar, suggesting that the average oxidation state of the Mo, V, and Te constituents are essentially retained during calcination. It is also evidenced from Table 4 that more $V^{4+}$ species (V2 $p_{3/2}$ BE = ca. 516.0 eV) could have been generated during the catalytic reaction.

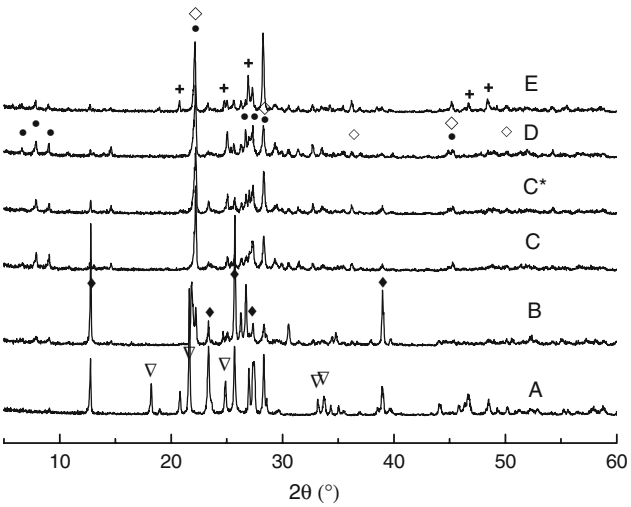


**Fig. 1** X-ray diffraction patterns of catalysts A–E. (◆ $MoO_3$, ● orthorhombic $Te_2M_{20}O_{57}$ ($M$ = Mo, V, and Nb), ◇ $Te_{0.33}MO_{3.33}$ ($M$ = Mo and V), ▽ $V_{3.6}Mo_{2.4}O_{16}$ and + $VOMoO_4$ phase)

### 3.2 XRD, Raman, and EPR

Over catalysts A and B (Fig. 1), one can detect intense peaks at $2\theta = 12.7$, 23.3, 25.6, 27.3 and 38.9° attributable to the $MoO_3$ phase (JCPDS 5-508). One can also detect $V_{3.6}Mo_{2.4}O_{16}$ phase (JCPDS 84-1952) in catalyst A. The detectable amount of $MoO_3$ in catalysts C, D, and E are low. A comparison between the XRD patterns of catalysts C and C* revealed that the amount of $MoO_3$ phase in C is lower than that in C*. The result suggested that the enhanced interaction among the Mo, V, and Te constituents in the preparation medium by ultrasonic treatment can effectively suppress phase segregation. The peaks at $2\theta = 6.6$, 7.9, 9.0° and the intense peaks at $2\theta = 22.1$, 26.6, 27.2, and 45.2° observed over catalysts C, D, and E are characteristics of orthorhombic $Te_2M_{20}O_{57}$ ($M$ = Mo, V) phase [20]. The peaks at $2\theta = 22.1$, 28.2, 36.2, 44.7 and 50.0° suggest the presence of $Te_{0.33}MO_{3.33}$ ($M$ = Mo and V) phase [22]. The peaks at $2\theta = 20.8$, 24.8, 27.0, 28.3, 46.8 and 48.5° observed over catalyst E ($\alpha = 1$) indicates the presence of $VOMoO_4$ (JCPDS18-1454), and this phase also exists in catalyst A. It seems that it is crucial to have the right amount of vanadium for the generation of the essential phase(s) in the MMO catalysts. According to Solsona et al. [23], the $VOMoO_4$ phase showed negative effect on catalytic activity in propane oxidation to AA. Based on the XRD results (Fig. 1), small amount of (V, Nb)-substituted $Mo_5O_{14}$ phases such as $(V_{0.07}Mo_{0.93})_5O_{14}$ and $(Nb_{0.09}Mo_{0.91})_5O_{14}$ could also be present in these catalysts. The free $MoO_3$ phase existing in the catalysts of low V content and the $VOMoO_4$ phase in the catalysts of high V content are thought to be adverse to propane oxidation to AA. On the other hand, the predominant M1 and

M2 phases in the Mo–V–Te catalysts of medium V content are crucial for propane oxidation to AA.

The Raman spectra acquired over the catalysts are shown in Fig. 2. The bands at 818 $cm^{-1}$ and 846 $cm^{-1}$ are ascribed to Mo–O vibration while the band at about 990 $cm^{-1}$ is assigned to Mo = O vibration of $MoO_3$ or $MoO_x$ oxide [34]. The weakening of the 818 $cm^{-1}$ and 990 $cm^{-1}$ signals in the C–E serial samples reflects the decline of these species with increasing V content. A broad band at around 885 $cm^{-1}$ is attributable to the stretching mode of bridging Mo–O–*M* (*M* = Mo, V) bonds of $Te_2M_{20}O_{57}$ [24], and the band at ca. 872 $cm^{-1}$ and that at 903 $cm^{-1}$ are attributable to distorted $Te_2M_{20}O_{57}$ and $VOMoO_4$ species, respectively. The band at ca. 885 $cm^{-1}$ dominates the Raman spectrum of catalyst D, suggesting that there is a high content of $Te_2M_{20}O_{57}$ in this catalyst. There is a band (shoulder) at ca. 906 $cm^{-1}$ observed over catalysts C* and E, indicating the existence of $VOMoO_4$ in the two catalysts. The Raman results are in good agreement with the XRD data.

The EPR results (Fig. 3) demonstrated that there are $Mo^{5+}$ species in the catalysts, and the $Mo^{5+}$ species are situated in distorted octahedral environment [29, 35, 36]. With increasing V content in the Mo–$V_\alpha$–Te–O samples ($\alpha$ = 0.4–1.0), the signal of $Mo^{5+}$ increases. The broadening of the paramagnetic bands is likely to be due to the presence of well-isolated $V^{4+}$ species [10]. The spectrum of catalyst E is notably different from that of the other catalysts. This is probably due to the fact that in catalyst E there is a large portion of $Mo^{5+}$ existing in the $VOMoO_4$ phase while in catalysts C and D most of $Mo^{5+}$ is present in the M1/M2 phases. Based on the results of Fig. 3b, one can deduce that the application of ultrasonic treatment can lead to enhanced presence of $Mo^{5+}$ species in catalyst C. Asakura et al. reported that the co-existence of $Mo^{5+}$ and $V^{4+}$ species is beneficial for propane partial oxidation to AA [11].

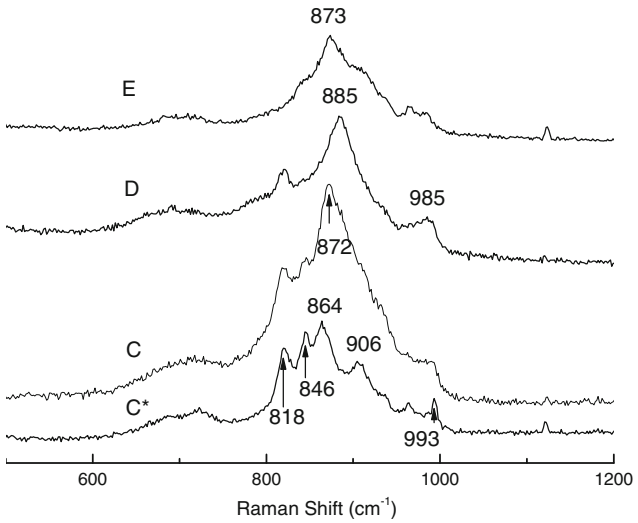


**Fig. 2** Raman spectra of catalysts C–E

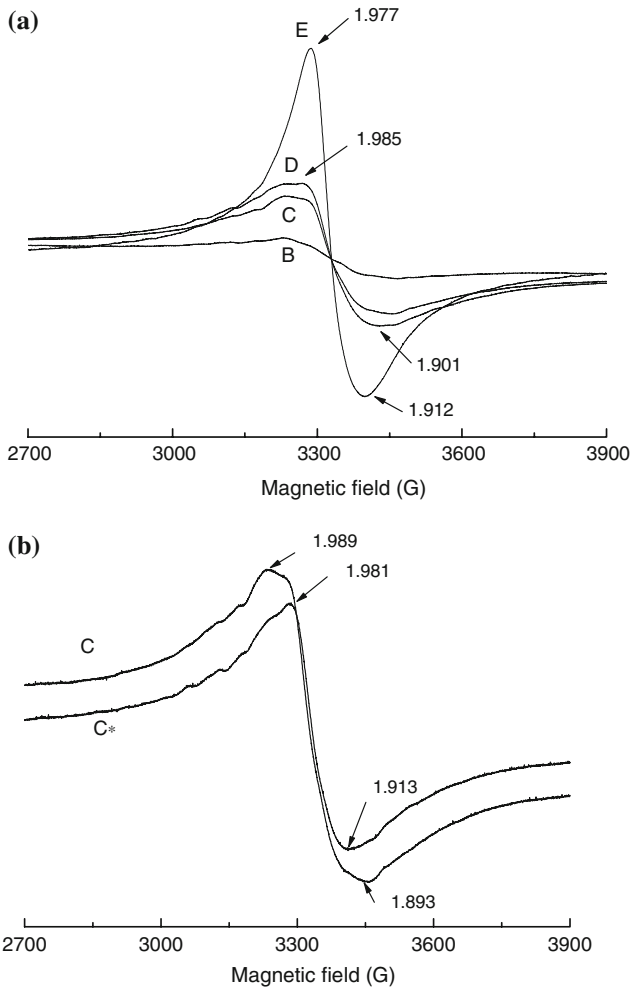


**Fig. 3** EPR spectra of (**a**) catalysts B–E, and (**b**) catalysts C and C*

### 3.3 $NH_3$-calorimetric, $H_2$-TPR, and SEM Results

Concepción et al. [37] and Baca et al. [38] investigated the strength of acidic sites of Mo–V–Te–Nb–O mixed metal oxide catalysts and found that the active catalysts present low Lewis and Brønsted acidity. Our Mo–V–Te–Nb–O catalysts prepared with ultrasonic treatment also showed similar tendency [31]. A comparison between the results obtained over catalysts C and C* reveals that with the ultrasonic treatment there is little effect on initial adsorption heat but on $NH_3$ coverage (Fig. 4). It is apparent that the overall surface acidity of catalyst C is enhanced as a result of ultrasonic treatment (C vs. C*). At high $NH_3$ coverage, the $NH_3$ probes can enter the channels of the M1 phase. The enhanced presence of M1 phase (XRD result) in the sample hence accounts for the rise in $NH_3$ adsorption capacity observed over catalyst C.

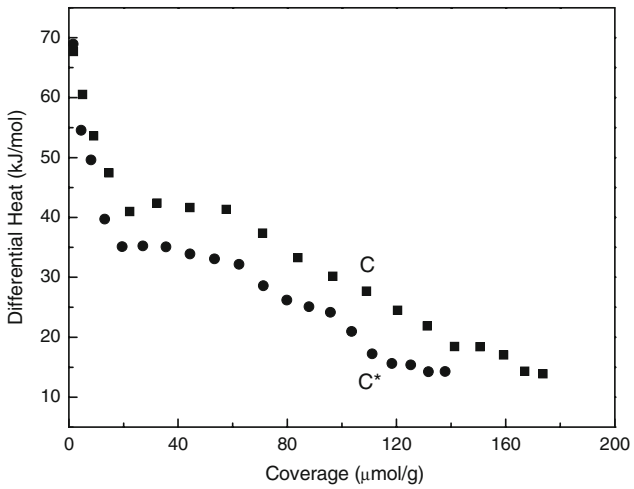


**Fig. 4** Differential adsorption heat versus $NH_3$ coverage over catalysts C and C*

The TPR profiles of representative samples of C and C* are shown in Fig. 5. Over catalyst C, the reduction peak is at 536 °C whereas over catalyst C*, it is at 553 °C. It is evident that the ultrasonic treatment leads to easy reduction of catalysts (C vs. C*); that is to say, a rise in activity of lattice oxygen. Similar tendency was observed over the ultrasonically treated Mo–V–Te–Nb catalysts [31].

The SEM images of C and C* are shown in Fig. 6. The rod-like morphology is usually ascribed to the orthorhombic phase [12, 25]. Figure 6 illustrated that the ultrasonic treatment would reduce the catalyst crystal size and result in enhanced presence of active plane of orthorhombic phase, which may also have an impact on the catalytic activity.

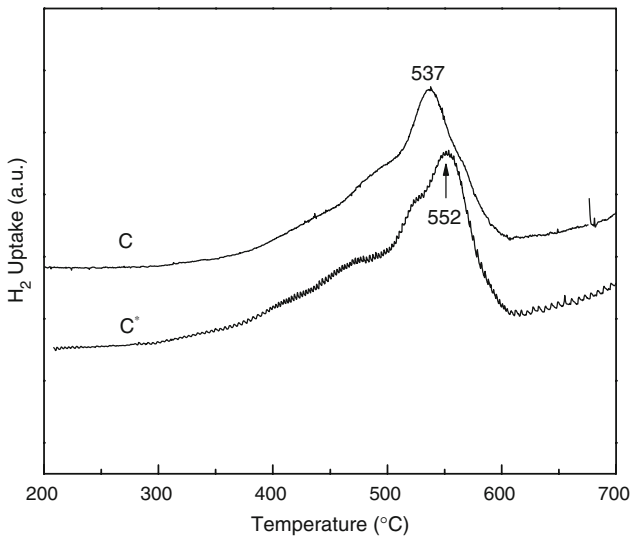


**Fig. 5** $H_2$-TPR profiles of catalysts C and C*

### 3.4 Catalytic Activity

The propane conversion, selectivity of products, and AA yield over the catalysts are depicted in Table 1. The introduction of water vapor of 40% by volume into the reaction feed is for the suppression of AA oxidation as well as for the stabilization of the oxidation state of partially reduced surface elements as illustrated by Guliants et al. [26]. Over $Mo_{1.00}V_{0.80}O_n$ (catalyst A) at 380 °C, the major products are propylene and carbon oxides ($CO_x$). Over catalysts B, C, and D (Mo–$V_\alpha$–Te–O, $\alpha = 0.40$, 0.60 and 0.80, respectively) at 400 °C, the products are AA, acrolein (minor), propylene, acetic acid, and carbon oxides. The propane conversion first increases with nominal (bulk) V content up to V/Mo = 0.6, and then decreases at higher nominal (bulk) V contents. Over catalysts B–D ($\alpha = 0.40$–0.80), relatively high AA selectivity was obtained; whereas over catalyst E ($\alpha = 1.00$), AA selectivity was drastically declined. It is worth noting that when the reaction temperature is decreased from 400 to 260 °C, high selectivity to acrolein (45.7%) and propylene (43.9%) are detected over catalyst E at the expense of propane conversion (4.8%) and AA yield (trace). The results reveal that the conversion of propane to AA involves the formation of propylene and acrolein as intermediates. As the V content of Mo–$V_\alpha$–Te–O catalysts increases from $\alpha = 0.40$ to $\alpha = 0.60$, the propane conversion increases from 13.2% to 48.4%. Referring to catalysts D and E, a slight change of V content from $\alpha = 0.80$ to $\alpha = 1.00$ results in significant change in product distribution. There is a small decline in propane conversion (from 48.4 to 39.5%) as the V content is raised from $\alpha = 0.60$ to $\alpha = 1.00$. Over catalyst C*, propane conversion, AA selectivity, and AA yield are 48.9%, 16.1% and 7.9%, respectively. The AA yield over catalyst C is 14.1%, significantly higher than that over catalyst C*. The AA selectivity observed over catalysts C and C* is 29.0% and 16.1%, respectively, and it is apparent that the ultrasonic treatment has notable effect on AA selectivity. The propane conversion over C is close to that over C*, and this is understandable in terms of the fact that similar consumption of $H_2$ was observed over C and C* in the TPR investigation. Catalyst D ($\alpha = 0.80$) shows an AA yield of 17.4% and an AA formation rate of 11.6 μmol $g^{-1}$ $min^{-1}$, which are the highest among the serial Mo–$V_\alpha$–Te–O catalysts ($\alpha = 0.40$–1.00). Guliants et al. also reported a promising performance obtained over a Mo–V–Te catalyst with the same Mo–V ratio but slightly higher content of Te [26]. Vitry et al. investigated the propane oxidation over the $Mo_6V_3Te_1$ catalyst and obtained an AA yield of 13.6% at 381 °C. Note that this $Mo_6V_3Te_1$ catalyst displayed significantly higher AA formation rate (2.96 mmol $g^{-1}$ $h^{-1}$), likely owing to the fact that the catalyst only consists of the pure M1 phase [30].

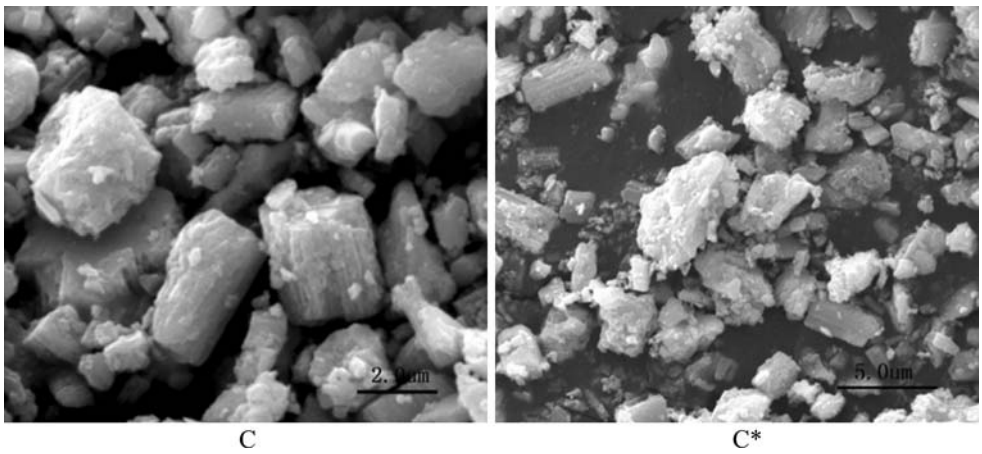


**Fig. 6** SEM image of catalyst C and C*

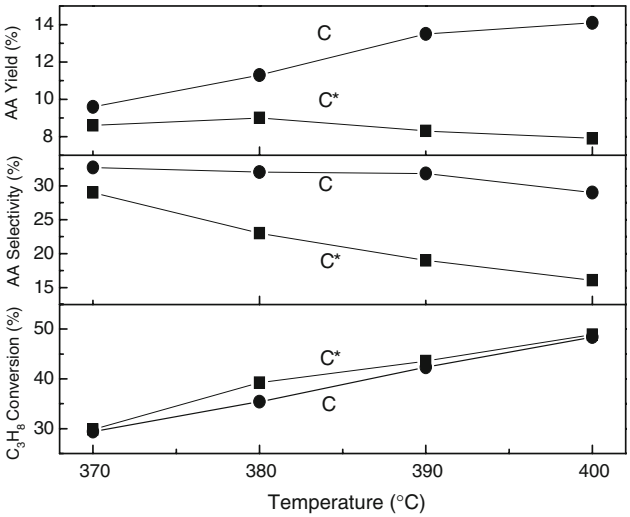


**Fig. 7** Propane conversion, AA selectivity and yield over catalysts C and C*

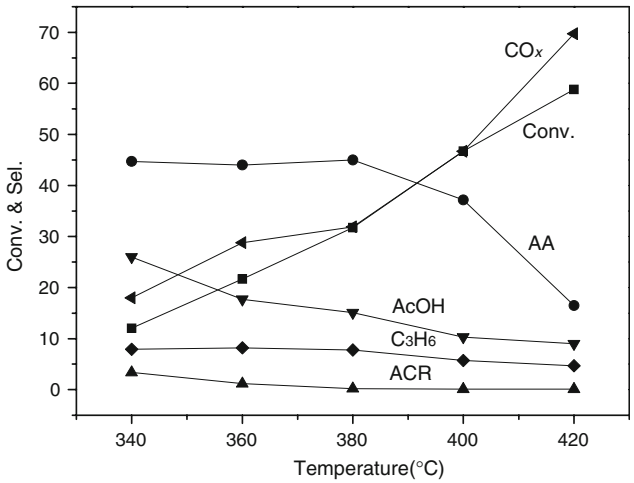


**Fig. 8** Performance of catalyst D versus temperature. (Reaction feed: propane/oxygen/steam/helium = 6/12/40/42 (volume ratio), catalyst amount: 1 g, W/F = 249 $g_{cat}$ h (mol $C_3H_8$)$^{-1}$

The effect of reaction temperature on propane conversion and product selectivity over catalysts C, C*, and D are depicted in Figs. 7 and 8. The conversion of propane and the selectivity to $CO_x$ increase with a rise in temperature, and understandably there is a decrease in AA selectivity. At elevated temperatures, C and C* showed similar propane conversion but the former is notably more selective to AA production. Over catalyst D, AA selectivity increases and reaches a maximum value of 45% at 380 °C. Below 360 °C, propane conversion is low whereas above 400 °C, deep oxidation of AA and intermediate products becomes significant. Thus the suitable temperature for AA generation is in the range of 380–400 °C. A rise in temperature from 340 to 380 °C would result in enhancement in $CO_x$ selectivity but little change in AA selectivity. When the temperature is further raised to 420 °C, there is a big decline in AA selectivity and a significant rise in $CO_x$ selectivity. The results also indicate that in the 340–380 °C range, the generation of $CO_x$ is not due to AA oxidation, but rather to the oxidation of intermediates such as acrolein or by-products such as acetic acid. In the 380–420 °C range, the formation of $CO_x$ is essentially originated from AA oxidation. The temperature dependence of catalytic performance is also strongly related to the kind of catalysts, for instance, at 260 °C propylene and acrolein are major products over catalyst E, and the tendency of having propylene and acrolein converted to other chemicals is low.

## 4 Discussion

The constituents of MMO catalysts show different functions in the partial oxidation of propane. It has been reported that V and Te are mainly for alkane and olefin activation, respectively [27, 39], whereas Mo is for oxygen insertion [40]. That orthorhombic $Te_2M_{20}O_{57}$ ($M$ = Mo,V,Nb) containing $Te^{4+}$, $Mo^{6+}/Mo^{5+}$, and $V^{5+}/V^{4+}$ entities are active and selective for propane oxidation to

AA has been reported by Santo et al. [13]. It is apparent that the Mo and V components are indispensable for the formation of the orthorhombic structure [22, 27], and an appropriate amount of V is essential for the generation of the $Te_2M_{20}O_{57}$ phase. Ueda et al. [14] suggested that the Te species locating at the central position of the hexagonal channels of $Te_2M_{20}O_{57}$ are effective in promoting the conversion of propylene intermediate to AA.

### 4.1 Effect of Ultrasonic Treatment

Ultrasonic treatment is commonly applied in synthetic processes as an effective means for dispersion enhancement of materials in liquid media. In the present study, we adopted the technique to enhance $TeO_2$ dispersion, and as a result, promoting the interaction of Te with the Mo, V constituents. The results of performance evaluation reflect the effectiveness of the approach. It has been observed that orthorhombic crystalline phase would be favorably formed in hydrothermal synthesis of MMO catalysts [14, 28, 29]. The generation of the orthorhombic phase, as revealed in the present study, can be facilitated effectively with the preparation mixture ultrasonically treated prior to the hydrothermal process. It is plausible that the ultrasonic waves enhance interaction of constituents in the liquid medium and hence promote component interaction and MMO precipitation. Furthermore, the ultrasonic treatment could result in surface enrichment of $Te^{4+}$ (XPS results, Tables 2 and 3) and generation of $Mo^{5+}$ (EPR data, Fig. 3), which in turn brings about the features that enable better catalyst activity and selectivity: (i) higher surface acidity ($NH_3$-calorimetric measurement, Fig. 4); and (ii) higher reactivity of lattice oxygen ($H_2$-TPR results, Fig. 5). A comparison study on the Mo–V–Te–Nb–O catalysts prepared with and without ultrasonic also showed a positive effect on the application of ultrasonic treatment [31].

### 4.2 Effect of Constitutional Elements

Solsona et al. reported the effect of elemental composition of Mo–V–Te–Nb–O catalyst prepared by slurry method on the development of crystalline active phase and consequently, the catalytic performance [23]. The activation of propane C–H bond is rate-determining in propane partial oxidation, and the V-sites ($V^{5+} = O \leftrightarrow {}^{4+}V^{\bullet}–O^{\bullet}$) [12] play an important role in propane activation [15, 30]. The V content in the Mo–V–Te–O catalysts has an impact on product distribution. As shown in Table 1, distinct product distributions of acrylic acid and carbon oxides can be observed over catalysts D and E, respectively. This suggests that a proper regulation of V content is crucial for the generation of the essential orthorhombic $Te_2M_{20}O_{57}$ (M1) ($M$ = Mo, V) phase which is active and selective for AA production. It was also revealed that the $MoO_3$ and $VOMoO_4$ phases nonselective to AA formation in propane oxidation [16] can be generated at lower (V/Mo < 0.6) or higher (V/Mo > 0.8) V content, respectively (Fig. 1). With V content in Mo–V–Te–O increasing from $\alpha = 0.40$ to $\alpha = 0.80$, the presence of $MoO_3$ phase declines (Fig. 1) whereas that of $Mo^{5+}$-containing species increases (Fig. 3). Considering that the AA yield over catalysts B, C, and D is 5.3%, 14.1%, and 17.4%, respectively (Table 1), one can presume that the presence of the $Mo^{5+}$ entities in the M1 ($Te_2M_{20}O_{57}$) and M2 ($Te_{0.33}MO_{3.33}$) phases is beneficial for AA production.

Catalysts B, C, and D show higher propane conversion than catalyst A, and the higher conversion is mainly due to the presence of the orthorhombic $Te_2M_{20}O_{57}$ phase. Note that the nature of catalyst (e.g. the V content and phase composition) as well as the operating condition (e.g. the reaction temperature) can have a drastic effect on the catalyst performance, for instance, catalyst C* showed high conversion but low selectivity at 400 °C in the present case (Table 1). It is more selective at low temperatures. It is known that the pair of electrons at a $Te^{4+}$-site can trigger allylic hydrogen abstraction of propylene to produce acrolein which then converts to AA via oxygen insertion [17]. The fact that propylene is the major product over catalyst A (one without Te) proves that Te presence is essential for the formation of acrolein and AA. As mentioned before, the ultrasonic treatment adopted in catalyst preparation improves the co-precipitation of the constituents and induces surface enrichment of $Te^{4+}$ at medium V content. The enrichment of surface Te-sites is thought to be beneficial for the improvement of AA selectivity.

## 5 Conclusion

In the present study, Mo–V–O and Mo–V–Te–O catalysts with various V content were synthesized hydrothermally with ultrasonic pretreatment. Detailed characterizations provide novel information on the physicochemical properties of the catalysts resulting from the systematic regulation of V content in catalyst and the adoption of ultrasonic treatment in catalyst preparation. The $MoO_3$ and $VOMoO_4$ phases nonselective to AA formation in propane oxidation are generated at low and high V content, respectively. It is revealed that a proper regulation of V content is required for the generation of active phases. In the fabrication of Mo–V–Te–O catalysts, the presence of Te in Mo–V–O promotes propylene conversion to AA via allylic hydrogen abstraction. Although the obtained acrylic yields of Mo–V–Te–O are less than that of Mo–V–Te–Nb–O, they are excellent in the Mo–V–Te–O category, thanks to the proper regulation of catalyst V content and the

adoption of ultrasonic treatment in catalyst preparation. The application of ultrasonic pretreatment would result in (i) enhancement of $Mo^{5+}$ species at the expense of free $MoO_3$ phase, (ii) surface enrichment of Te at medium V content, (iii) enhancement in reactivity of lattice oxygen, surface acidity, and formation of orthorhombic phase. These catalyst features brought about by the improved preparation methodology account for the enhanced AA yield. The approach of ultrasonic treatment could also be applied to the fabrication of other multi-component catalysts where high uniformity of constituents is required.

**Acknowledgments** We thank NSFC (20673052), HKBU (FRG/03-04/II-17), and JSNSF (BK2006112) for financial supports.

## References

1. Centi G, Trifirò F, Ebner JR, Franchetti VM (1988) Chem Rev 88:55
2. Nojiri N, Sakai Y, Watanabe Y (1995) Catal Rev 37:145
3. Landi G, Lisi L, Volta JC (2004) J Mol Catal A 222:175
4. Landi G, Lisi L, Russo G (2005) J Mol Catal A 239:172
5. Li XK, Zhao J, Ji WJ, Zhang ZB, Chen Y, Au CT, Han S, Hibst H (2006) J Catal 237:58
6. Ushikubo T, Oshima K, Kayou A, Hatano M (1997) Stud Surf Sci Catal 112:473
7. Ushikubo T, Nakamura H, Koyasu Y, Wajiki S (1995) US Patent 5 380 933
8. Gaffney AM, Chaturvedi S, Clark MB Jr, Han S, Le D, Rykov SA, Chen JG (2005) J Catal 229:12
9. Watanabe H, Koyasu Y (2000) Appl Catal A: Gen 194–195:479
10. Baca M, Millet JMM (2005) Appl Catal A: Gen 279:67
11. Asakura K, Nakatani K, Kubota T, Iwasawa Y (2000) J Catal 194:309
12. Grasselli RK, Burrington JD, Buttrey DJ, DeSanto P Jr, Lugmair CG, Volpe AF Jr, Weingand T (2003) Top Catal 23:5
13. de Santo P Jr, Buttrey DJ, Grasselli RK, Lugmair CG, Volpe AF, Toby BH, Vogt T (2003) Top Catal 23:23
14. Ueda W, Vitry D, Katou T (2005) Catal Today 99:43
15. Grasselli RK (2005) Catal Today 99:23
16. Novakova EK, Vedrine JC (2006) In: Fierro JLG (ed) Metal oxides: chemistry and applications. CRC Press, Boca Raton, 413 pp
17. Grasselli RK (2001) Top Catal 15:93
18. Lin MM (2003) Appl Catal A: Gen 250:287
19. Lin MM (2003) Appl Catal A: Gen 250:305
20. Oshihara K, Hisano T, Ueda W (2001) Top Catal 15:153
21. Vitry D, Morikawa Y, Dubois JL, Ueda W (2003) Appl Catal A: Gen 251:411
22. Botella P, López Nieto JM, Solsona B (2002) Catal Lett 78:383
23. Solsona B, López Nieto JM, Oliver JM, Gumbau JP (2004) Catal Today 91–92:247
24. Holmesa SA, Al-Saeedi J, Guliants VV, Boolchand P, Georgiev D, Hackler U, Sobkow E (2001) Catal Today 67:403
25. Feng RM, Yang XJ, Ji WJ, Zhu HY, Gu XD, Chen Y, Han S, Hibst H (2007) J Mol Catal A 267:245
26. Guliants VV, Bhandari R, Al-Saeedi JN, Vasudevan VK, Soman RS, Guerrero-Pérez O, Bañares MA (2004) Appl Catal A: Gen 274:123
27. Botella P, López Nieto JM, Solsona B, Mifsud A, Marquez F (2002) J Catal 209:445
28. Vitry D, Dubois JL, Ueda W (2004) J Mol Catal A 220:67
29. Botella P, Solsona B, Martinez-Arias A, López Nieto JM (2001) Catal Lett 74:149
30. Vitry D, Morikawa Y, Dubois JL, Ueda W (2003) Top Catal 23:47
31. Yang XJ, Feng RM, Ji WJ, Au CT (2008) J Catal 253:57
32. Moulder JF, Stickle WF, Sobol PE, Bomben KD (1995) Handbook of X-ray photoelectron spectroscopy. Physical Electronics, Inc., Minnesota
33. Hayashi H, Shigemoto N, Sugiyama S, Masaoka N, Saitoh K (1993) Catal Lett 19:273
34. Banares MA, Hu H, Wachs IE (1995) J Catal 155:249
35. Dyrek K, Che M (1997) Chem Rev 97:305
36. Novakova EK, Vedrine JC, Derouane EG (2002) J Catal 211:235
37. Concepción P, Botella P, López Nieto JM (2004) Appl Catal A: Gen 278:45
38. Baca M, Pigamo A, Dubois JL, Millet JMM (2005) Catal Commun 6:215
39. Thorsteinson E, Wilson T, Young F, Kasai P (1978) J Catal 52:116
40. Grasselli RK (1999) Catal Today 49:141